Evaluation of the Position and Function of Aqueous Drainage Implants With Magnetic Resonance Imaging

Efstathios T. Detorakis, MD, PhD, Thomas Maris, PhD,† Efrosini Papadaki, MD, PhD,† Miltiadis K. Tsilimbaris, MD, PhD,* Apostolos H. Karantanas, MD, PhD,† and Ioannis G. Pallikaris, MD, PhD**

Purpose: To evaluate position and function of antiglaucomatous Ahmed and Molteno shunts using magnetic resonance imaging with head and surface coils.

Methods: Eight patients (5 males) with shunt implants were included, 4 with Ahmed (FP-7) and 4 with Molteno (s1, single plated). All patients were operated at least 6 months before imaging. In 3 cases (2 with Molteno and 1 with Ahmed shunt), the intraocular pressure (IOP) was above 21 mm Hg, despite maximal medical treatment. The shunt endplate, tube and filtering blebs were identified in T1-weighted and T2-weighted images with both head and surface coils. Volumetric measurements of the orbits, eyeball, and filtering bleb and calculation of the endplate position along sagittal, transverse, and vertical axes were performed in T1-weighted and T2-weighted images using head coils.

Results: The shunt endplate was identified in T1-weighted and T2-weighted images (head coils) as a low intensity (dark) circumlinear band at the superotemporal aspect of the eyeball, surrounded by a pocket of water density, corresponding to the filtering bleb. The anterior position of the endplate, and smaller volume of the orbital cavity (less available orbital space) were associated with higher IOP. Filtering bleb volume was inversely correlated with IOP. In the unsuccessful cases, filtering bleb was absent.

Conclusions: Magnetic resonance imaging provides insights into the mechanism of aqueous outflow and causes of failure of shunts. A lower orbital volume is associated with anterior position of the shunt endplate and poor shunt performance.

Key Words: MRI, glaucoma, shunts, orbit, aqueous

(*J Glaucoma* 2009;18:453–459)

Aqueous drainage implants (shunts) are devices implanted to eyes with uncontrolled intraocular pressure (IOP), aiming at establishing a sufficient aqueous humor outflow.[1,2] Shunts are commonly made of silicone or acrylic polymers.[2,3] Various designs have so far been proposed, generally divided into nonvalved mechanisms (such as Baerveldt[4] and Molteno[5]) and valved mechanisms (such as Ahmed[6] and Krupin[7]), the latter containing a true valve mechanism, which theoretically allows outflow of aqueous only when IOP rises above a predetermined value.[1,6,7] Shunt implantation can be complicated by hypotony, migration, erosion or extrusion through the overlying conjunctiva and corneal decompensation.[1] Furthermore, failure to control the IOP can be observed either early postoperatively (often attributed to obstruction of the tube by fibrin, blood, iris, or silicone oil)[1,6] or later (often caused by the development of a thick fibrous capsule, which may require needling or more extensive reconstructive surgery).[8,9]

Magnetic resonance imaging (MRI) is a noninvasive technique, extensively used in the study of ocular and orbital tissues.[10–12] Standard MRI studies of the orbits are performed with head coils whereas surface coils enable imaging of superficial structures, such as the eyeball.[13] A previous study has employed high resolution MRI with head coils in pediatric patients with Ahmed implants, to evaluate indications for reoperation in cases of failure.[14] The present study employs high resolution MRI with head and surface coils to evaluate adult patients with successful and unsuccessful Ahmed and Molteno implants. Results could prove useful in understanding mechanisms of failure of Ahmed and Molteno implants in adult patients and in establishing MRI based indications for surgical revision.

MATERIALS AND METHODS

This is a retrospective nonrandomized case series. Eight patients in whom a shunt had been implanted (the tube inserted into the anterior chamber) in 1 eye were included. Patients were recruited from the Glaucoma Service of the Department of Ophthalmology of the University Hospital of Heraklion, Crete, Greece. The shunt was an Ahmed type (model FP7, New World Medical Inc, Rancho Cucamonga, CA) in 4 cases and a single-plated Molteno type in 4 cases (model S1, Molteno Ophthalmic Ltd, Dunedin, New Zealand). The demographic and clinical information of patients studied, including age, sex, indication for shunt implantation, postoperative interval, level of IOP, axial length and antiglaucomatous medications used are presented in Table 1. All patients signed a written informed consent form in accordance with the tenets of the Declaration of Helsinki.

All patients were operated by the same surgeon (E.T.D.) with the same technique. Under topical (subconjunctival) anesthesia, a large fornix-based conjunctival flap was created at the superotemporal quadrant of the ocular surface. The implant patency was confirmed in all cases before insertion by irrigating the tube with normal saline using a 27 G cannula. The implant endplate was then inserted into the subconjunctival pocket and sutured on the scleral surface with 2 nonabsorbable 6.0 sutures. The anterior chamber was then entered with a 23 G needle with a direction parallel to the anterior iris surface, at a limbal

Received for publication January 8, 2008; accepted August 2, 2008.
From the Departments of *Ophthalmology; and †Medical Imaging, University Hospital of Heraklion, Crete, Greece.
Conflict of Interest: None for all authors.
Reprints: Efstathios T. Detorakis, MD, PhD, Department of Ophthalmology, University Hospital of Heraklion, 71110 Stavrakia, Heraklion, Crete, Greece (e-mail: detorakis@hotmail.com).

DOI:10.1097/IJG.0b013e3181895e42

TABLE 1. Demographic and Clinical Information of Patients Studied

Patient	Age	Sex	Clinical Condition	Shunt Type	Axial Length (mm)	Interval (mo)	IOP (mm Hg)	Antiglaucomatous Medications
1	32	Male	Aphakic glaucoma	Ahmed	29.4	6	12	None
2	70	Male	Multiple failed trabeculectomies, pseudophakia	Molteno	24.1	12	15	None
3	54	Male	Multiple failed Trabeculectomies	Molteno	26.7	18	24	Latanoprost, timolol
4	64	Female	Multiple failed trabeculectomies, pseudophakia	Ahmed	24.5	5	12	None
5	27	Female	Multiple failed trabeculectomies, aphakia	Molteno	28.2	6	37	Latanoprost, timolol, dorzolamide
6	75	Male	Neovascular glaucoma	Ahmed	23.3	8	18	None
7	65	Female	Neovascular glaucoma	Ahmed	25.0	9	40	Latanoprost, timolol, acetazolamide PO
8	88	Male	Multiple failed trabeculectomies, pseudophakia	Molteno	23.9	15	14	None

IOP indicates intraocular pressure.

site corresponding to the implant plate. The implant tube was trimmed accordingly and inserted (bevel-up) into the anterior chamber. The position of the tube into the chamber was examined, and if found satisfactory (adequate clearance to corneal endothelium and adequate length), the tube was anchored to sclera with a U-shaped 6.0 nonabsorbable suture, adjacent to the implant plate. In the case of Molteno shunts, a 6.0 vicryl suture was used to ligate the tube to prevent against early postoperative hypotony. The episcleral portion of the tube was then covered with a patch of cadaveric preserved human pericardium (Tutoplast, Tutogen Medical GmbH, Neunkirchen, Germany), which was anchored to the sclera with 7.0 interrupted absorbable sutures. The conjunctiva was closed also with 7.0 interrupted absorbable sutures. The insertion of the shunt in all cases studied was not associated with any significant postoperative complication, such as corneal decompensation, exposure or extrusion of the implant tube or endplate. In the case of Molteno shunts, patients were prescribed acetazolamide PO for the first 3 postoperative months (until the complete absorption of the ligating suture). In 5 cases (3 cases with Ahmed shunt and 2 cases with Molteno shunt), the insertion was successful, resulting in satisfactory IOP control without any antiglaucomatous medications. In 3 cases (1 case with Ahmed shunt and 2 cases with Molteno shunt), the insertion was unsuccessful, resulting in elevated IOP despite the maximal use of topical and oral antiglaucomatous medications. In the unsuccessful cases, biomicroscopic examination of the tube into the anterior chamber did not reveal the presence of material obstructing the lumen (such as debris or vitreous). Furthermore, in both successful and unsuccessful cases, biomicroscopic examination over the area of the shunt endplate revealed a prominent conjunctival elevation.

Each patient underwent high-resolution, T1-weighted and T2-weighted MRI scanning using a 1.5-T scanner (SonataVision, Siemens Medical Solutions, Erlangen, Germany). All MRI studies were performed at least 6 months after shunt implantation, to allow for a complete healing of conjunctiva and orbital tissues and absorption of the ligating suture (in the case of Molteno shunts). Images were obtained using both head coils and ocular surface coils. For the later technique, an array of surface coils was deployed over the orbit in a mask-like closure held strapped to the face. Subjects were repeatedly coached to avoid unnecessary movements during scanning. Blinking was reduced by maximizing precorneal humidity using a transparent facemask and instructing subjects to avoid unnecessary blinks. Head movement was minimized by secure stabilization to the surface coil facemask and judicious use of padded restraints. Axial, coronal, and sagittal images were obtained at 2 mm thickness using a 256×224 matrix over a 18.3×21.0 cm field of view. DICOM images were analyzed with the efilm workstation (eFilm Medical Inc, Toronto, Ontario, Canada) and the EvoRAd RIS-PACS workstation (EvoRAd Medical Information Systems, Heraklion, Crete, Greece). Only images free from degradation by motion or other artifacts were analyzed quantitatively. All images were analyzed by the same experienced examiner (E.P.) who was masked against clinical information of the patients studied.

The shunt endplate was identified as a circumlinear structure with a low intensity (dark) in both T1-weighted and T2-weighted images, located adjacent to the sclera at the superotemporal aspect of the eyeball. The position of the endplate, in relation to the orbital cavity, along the sagittal, transverse, and vertical axes was evaluated by measuring the minimal distance between the edge of the shunt endplate and the orbital apex, the superior orbital wall (along an axis parallel to the interhemispheric fissure) and the lateral orbital wall (along an axis perpendicular to the interhemispheric fissure), in T1-weighted images placed nearest to the midline of the implant, using head coils (Figs. 1, 2). The position of the shunt endplate along the sagittal axis was evaluated in sagittal images whereas the position along the transverse and vertical axes was evaluated in coronal images. The position of the shunt tube and its course into the anterior chamber was evaluated in T2-weighted coronal images placed along the anterior surface of the globe using surface coils (Fig. 3). The episcleral portion of the implant tube was examined in T2-weighted sagittal images also using surface coils.

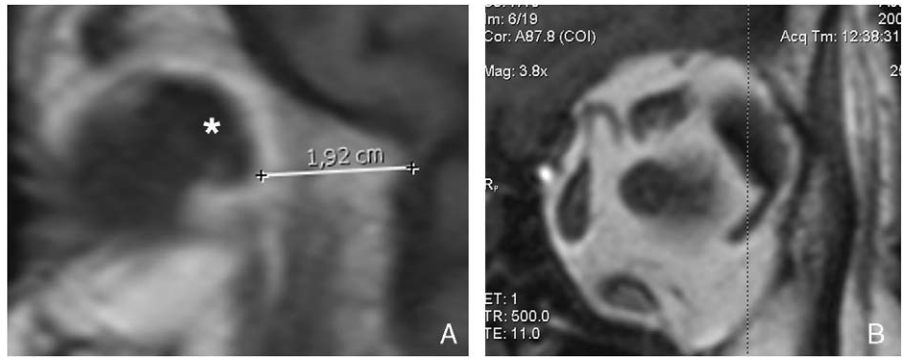

FIGURE 1. Evaluation of the implant plate position along the sagittal axis by measuring the minimal distance between the implant endplate (*) and the orbital apex, in sagittal T1-weighted sections (A) through the midline of the implant (as shown in the respective coronal section B), using head coils (patient 6).

The volume of the orbital cavity and eyeball were also measured in T1-weighted coronal images (Fig. 4). The eyeball volume was subtracted from the orbital cavity volume and the difference recorded as effective orbital volume (EOV), to provide an estimation of the available space in the orbital cavity for the implantation of the shunt (Fig. 5). The filtering bleb, identified as a pocket of water signal (high intensity in T2-weighted images and low intensity in T1-weighted images) was also evaluated using head coils in T2-weighted axial images and its volume measured (Fig. 4). All volumetric calculations were performed by summing the cross-sectional area of each structure in every coronal section in which it was visible and multiplied by the plane thickness, as previously described.[13]

Differences in the implant plate position along the sagittal, transverse, and vertical axes and also in filtering bleb volume, orbital volume, eyeball volume, and EOV between successful cases and unsuccessful cases were examined (independent samples *t* test). Furthermore, differences in the position of the implant plate along the vertical, sagittal, and transverse axes and also in the filtering bleb volume between Ahmed and Molteno shunts were examined (independent samples *t* test). Correlations between the implant plate position and the postoperative interval and patients' age were also examined (Pearson bivariate correlations coefficient, independent samples *t* test). Statistical analysis of findings was performed using SPSS 8.0 (SPSS, Chicago, IL). Statistical significance was set at 0.05.

RESULTS

The shunt endplate was identified in all cases as a curvilinear very low-density (dark) band in both T1-weighted and T2-weighted images, located at the superotemporal scleral quadrant. Adjacent to the implant endplate, the filtering bleb area was identified as a pocket of variable size, corresponding to high intensity in T2-weighted images and low intensity in T1-weighted images with head coils, in 6 cases. In 2 cases (1 case with Ahmed shunt and 1 case with Molteno shunt) the filtering bleb was not present, despite the fact that slit-lamp biomicroscopy revealed a prominent elevation of the conjunctiva covering the endplate. MRI with surface coils (T2-weighted coronal images) was successful in delineating the shunt endplate (adjacent to the sclera) and the portion of the implant tube (located into the anterior) chamber in all cases. On the contrary, clear delineation of the episcleral portion of the tube along its entire length with sagittal T2-weighted images was not possible in any case.

The filtering bleb volume and the implant endplate position along the vertical, transverse, and sagittal axes did

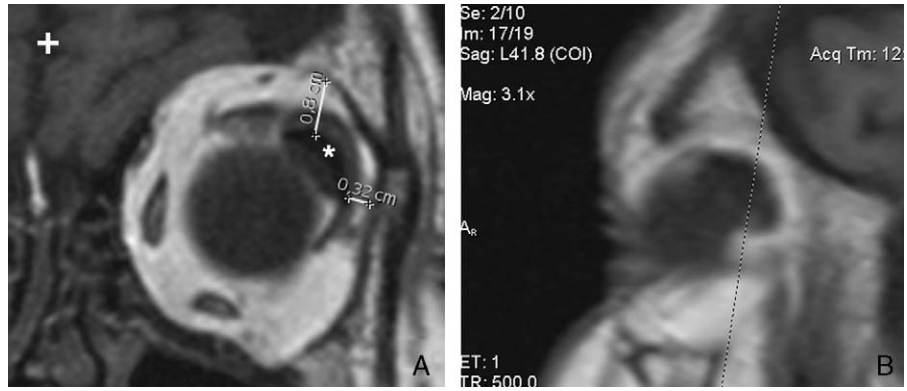

FIGURE 2. Evaluation of the position of the implant endplate (*) along the transverse and vertical axes by measuring the minimal distance between the endplate and the superior orbital wall and also the minimal distance between the endplate and the lateral orbital wall (along axes parallel and perpendicular to the interhemispheric fissure, respectively), in T1-weighted coronal sections (A) through the midline of the implant (as shown in the respective sagittal section B), using head coils. The interhemispheric fissure is shown with + (patient 6).

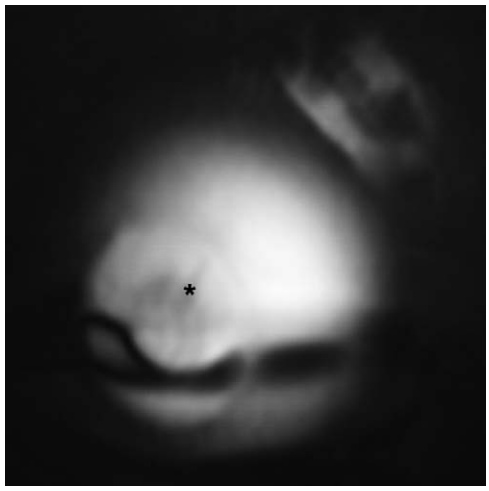

FIGURE 3. Evaluation of the implant tube (*) into the anterior chamber in a T2-weighted coronal section with surface coils (patient 1).

not differ significantly between Ahmed and Molteno implants (Table 2). Furthermore, the implant plate position along the vertical and transverse axes was not significantly different between successful and unsuccessful cases (Table 2). On the contrary, filtering bleb volume was significantly larger in successful, compared with unsuccessful cases, whereas the distance from orbital apex of the implant plate in the sagittal plane was significantly lower (implying more posterior plate position) for successful cases, compared with unsuccessful ones (Table 2).

Orbital volume and EOV were significantly higher in successful, compared with unsuccessful cases, whereas the respective difference concerning eyeball volume was statistically not significant (Table 3). The correlations between the implant plate position along the vertical, transverse, or sagittal axes and the postoperative interval or patients' age were statistically not significant.

DISCUSSION

Previous studies have employed various imaging modalities, including plain radiographs,[15] high frequency ultrasound biomicroscopy (UBM)[16,17] and MRI[14,18] for the examination of Ahmed and Baerveldt shunt implants. This study evaluated successful and unsuccessful silicone Ahmed (FP-7) and single-plated Molteno shunts in adult patients by employing MRI with both head coils and surface coils. Results suggest that MRI scans can be used to evaluate the filtering bleb and thus the aqueous drainage into the orbital tissues. Results also suggest that anterior position of the shunt plate may be associated with decreased orbital volume and poor IOP control.

A previous study has reported that MRI may help in understanding causes of elevated IOP in the presence of an Ahmed shunt in pediatric patients, as the filtering bleb surrounding the shunt endplate can be evaluated.[14] Results from the present study also imply that MRI can be used to examine shunt position and function in adult patients. As previously described, shunt endplate material appeared as a low signal (dark) curvilinear band at the superotemporal aspect of the globe, separating pockets of water signal (low in T1-weighted images and high in T2-weighted images), which corresponded to the aqueous within the shunt

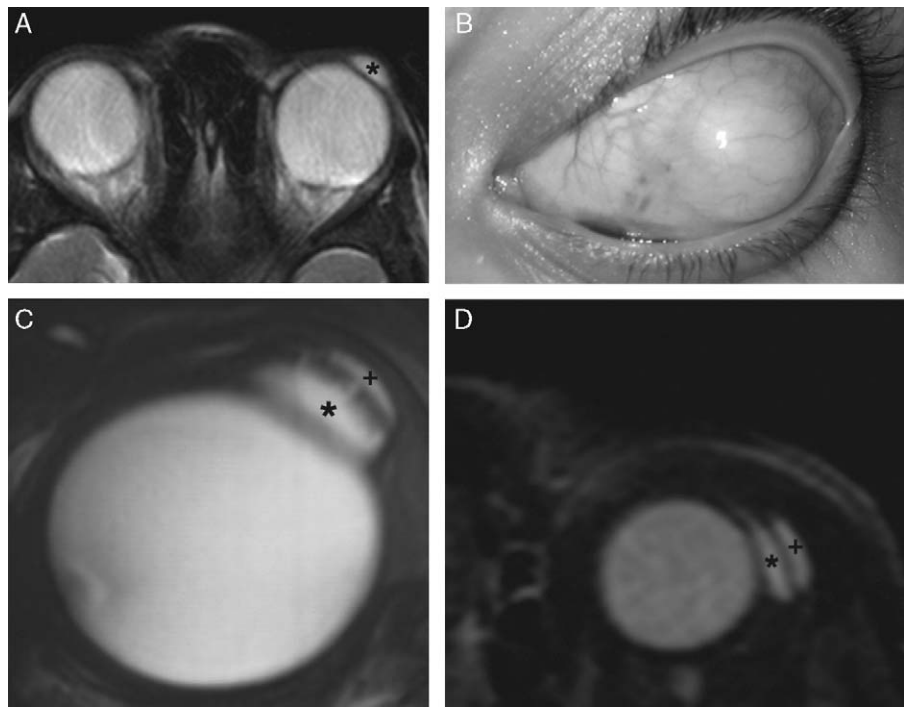

FIGURE 4. Absent filtering bleb in a failed shunt implant (patient 5) evaluated with T2-weighted transverse images (A), despite a prominent elevation of conjunctiva corresponding to the implant plate (B). Well-formed filtering blebs (+) in successful cases, evaluated with T2-weighted transverse images with surface coils (C, patient 1) and head coils (D, patient 2). The shunt endplate is marked with *.

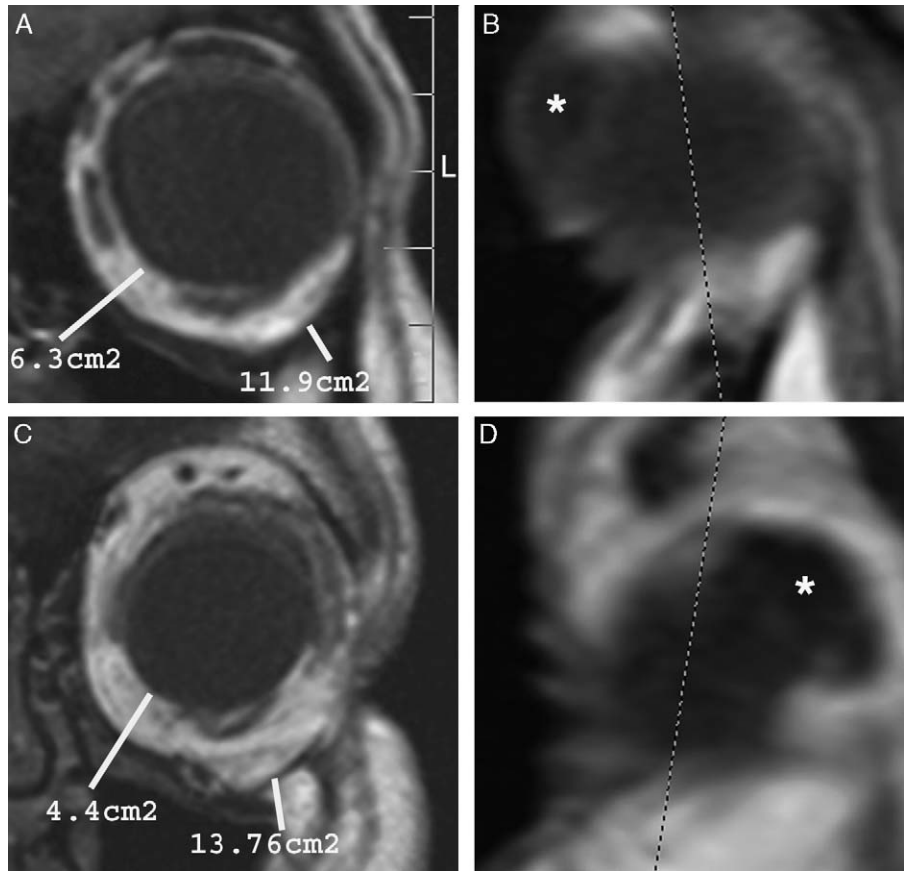

FIGURE 5. Different orbital and eyeball areas in 2 patients (presented in coronal images A and C, respectively), in sections through the eyeball equator (as shown in corresponding sagittal images B and D). The areas of the orbital and eyeball sections are shown in cm^2. In the patient shown in A and B (patient 5), EOV was less (14.2 mL), compared with the patient shown in C and D (patient 6, 22.6 mL). The shunt endplate (marked with * in sagittal images B and D) was anteriorly positioned in the former case, compared with the latter.

endplate and at the filtering bleb.[18] The absence or poor formation of a filtering bleb surrounding the implant endplate was invariably associated with poor IOP control in the cases examined in the present study, whereas the volume of the filtering bleb was inversely correlated with the achieved level of IOP. An increased distance between the posterior aspect of the implant body and the orbital apex (implying anterior position of the implant endplate) was also associated with poor IOP control (and poorly formed filtering blebs). This finding could possibly be explained by the compression of the implant endplate owing to proximity to muscle insertions, as previously suggested.[14] The correlations between anterior shunt endplate position (associated with poor shunt function) and decreased orbital volume and decreased EOV possibly reflect the limited available space for the shunt and the filtering bleb into a tight orbit. This correlation also implies that MRI may be used to provide orbital volumetric calculations before the shunt insertion so that use of a smaller (pediatric) shunt implant might possibly be considered in adult orbits with decreased volumes. Interestingly, correlations between the endplate position along the vertical and transverse axes and the orbital volume were statistically not significant. Although this finding may be attributed to anatomic factors, it may also reflect the fact that the orbital apex (used in the measurements of distances along the sagittal axis) is a more stable landmark than the superior and lateral orbital walls (used in the measurements of distances along the transverse and vertical axes). The fact that the endplate position was not correlated with the postoperative interval advocates against a progressive late migration and rather implies that endplate position is

TABLE 2. Filtering Bleb Volume (Mean ± SD) and Distance of the Valve Implant Plate From Anatomic Landmarks at the Sagittal, Transverse, and Vertical Axes in Ahmed and Molteno Type Implants and also in Successful and Unsuccessful Cases and Statistical Significance of Respective Differences (Independent Samples *t* test)

Parameter	Ahmed	Molteno	*P*	Successful	Unsuccessful	*P*
Filtering bleb volume (mm^3)	0.24 ± 0.10	0.18 ± 0.14	0.47	0.29 ± 0.18	0.09 ± 0.04	≈0.00
Sagittal distance (mm)	20.31 ± 4.70	19.75 ± 5.24	0.18	16.52 ± 1.14	27.97 ± 2.28	0.01
Transverse distance (mm)	3.65 ± 2.48	3.84 ± 2.97	0.39	3.42 ± 3.35	3.91 ± 3.32	0.45
Vertical distance (mm)	7.77 ± 1.92	7.05 ± 3.30	0.17	7.68 ± 2.14	7.22 ± 1.78	0.24

TABLE 3. Orbital Volume, Eyeball Volume, and EOV (Mean ± SD) in Successful and Unsuccessful Cases and Statistical Significance of Respective Differences (Independent Samples *t* test)

Parameter	Successful Cases	Unsuccessful Cases	*P*
Orbital volume (mL)	27.14 ± 2.10	22.15 ± 1.36	0.04
Eyeball volume (mL)	6.31 ± 2.73	7.24 ± 3.57	0.22
EOV (mL)	20.89 ± 2.11	14.90 ± 1.93	0.03

EOV indicates effective orbital volume.

stabilized early in the postoperative course. The mean filtering bleb volume did not differ significantly between Molteno and Ahmed shunts, although the endplate area differs between them (184 mm^2 in the Ahmed implant and 129 mm^2 in the single-plated Molteno implant),[15] implying that bleb volume may be associated with patient-related parameters, such as the orbital volume, rather than with shunt implant type.

Findings also imply that MRI with surface coils is of limited value in the study of shunt implants. The fact that the episcleral portion of the tube was not delineated along its entire length with surface coils images may possibly be attributed to the oblique course of the tube along a quasi-sagittal (rather than sagittal) axis. Perhaps the episcleral portion of the tube, possible peritubular leak and alterations in the tube course such as a kink potentially affecting aqueous outflow, may be more accurately examined with UBM, as previous studies have suggested.[16,17,19] It has previously been proposed that contrast enhancement with gadolinium should be performed in the MRI studies of shunt implants, as extensive contrast enhancement around the implant endplate was correlated with scar tissue around the shunt plate and poor filtering outflow.[14] Accordingly, surgical debulking of the scar tissue around the implant plate in such cases was successful in restoring filtering activity.[14] In the present study, delineation of the implant endplate and filtering bleb from the surrounding orbital tissues and detection of shunt endplate position were satisfactory, especially with T2-weighted images, without the administration of gadolinium, implying that the MRI study of most shunt implants may be performed in a less invasive manner. The administration of a contrast enhancing agent may be reserved for the differentiation between endplate malfunction and endplate encapsulation, necessitating replacement of the shunt or surgical needling or debulking, respectively, as previously suggested.[14]

Apart from understanding the mechanisms of aqueous drainage by shunts and providing information for improvements in the design of such implants, MRI studies may be also have direct clinical implications, especially in the decision-making for the appropriate treatment in cases with poor IOP control. High IOP despite a well-formed filtering bleb around the implant endplate in MRI (and thus a functioning implant) could be attributed to small implant size (inadequate filtering area), which would be an indication for insertion of a second (additional) shunt implant. On the other hand, high IOP with a poorly formed or totally absent filtering bleb in MRI would imply shunt failure. This could be attributed to tube obstruction by vitreous, debris, or iris[17] (usually visible in direct biomicroscopic or UBM examination and possibly treatable with YAG-laser lysis of obstructing material[20] or tube irrigation[8]), or to plate malfunction or encapsulation, necessitating replacement of the implant, or surgical debulking or needling of encapsulating tissue.[14,21]

The relatively small number of cases examined and the nonrandomized retrospective recruitment limit the strength of this study. On the other hand, the fact that all cases were operated by the same surgeon and were examined with the same MRI techniques and by the same experienced examiner and the fact that findings were highly reproducible possibly enhance the validity of results. Two popular shunt designs were included in equal numbers to enable a comparison between them concerning filtering bleb volume and endplate position, despite the fact that the selection of only 1 type would render the population study homogeneous and strengthen its statistical power. The importance of MRI in the study of shunt implants may be even more pronounced for implants inserted through the pars plana, as direct visualization of the tube is more difficult in such cases. Future research in this area may include the examination of the rate of aqueous flow through the implant tube by employing specialized MRI techniques, such as the phase contrast imaging, already in use for the measurement of cerebrospinal fluid outflow.[22,23]

REFERENCES

1. Sidoti PA, Baerveldt G. Glaucoma drainage implants. *Curr Opin Ophthalmol*. 1994;5:85–98.
2. Ayyala RS, Harman LE, Michelini-Norris B, et al. Comparison of different biomaterials for glaucoma drainage devices. *Arch Ophthalmol*. 1999;117:233–236.
3. Ayyala RS, Michelini-Norris B, Flores A, et al. Comparison of different biomaterials for glaucoma drainage devices. *Arch Ophthalmol*. 2000;118:1081–1084.
4. Lloyd MA, Baerveldt G, Heuer DK, et al. Initial clinical experience with the Baerveldt implant in complicated glaucomas. *Ophthalmology*. 1994;101:640–650.
5. Molteno AC. New implant for drainage in glaucoma: clinical trial. *Br J Ophthalmol*. 1969;53:606–615.
6. Ayyala RS, Zurakowski D, Smith JA, et al. A clinical study of the Ahmed glaucoma shunt implant in advanced glaucoma. *Ophthalmology*. 1998;105:1968–1976.
7. Krupin T, Ritch R, Camras CB, et al. A long Krupin-Denver shunt implant device attached to a 180 degrees scleral explant for glaucoma surgery. *Ophthalmology*. 1988;95:1174–1180.
8. Krawitz PL. Treatment of distal occlusion of Krupin eye shunt with disk using cannular flush. *Ophthalmic Surg*. 1994;25:102–104.
9. Chen PP, Palmberg PF. Needling revision of glaucoma drainage device filtering blebs. *Ophthalmology*. 1997;104:1004–1010.
10. Ainbinder DJ, Haik BG, Mazzoli RA. Anophthalmic socket and orbital implants. Role of CT and MR Imaging. *Radiol Clin North Am*. 1998;36:1133–1147.
11. Ozgen A, Aydingoz U. Normative measurements of orbital structures using MRI. *J Comput Assist Tomogr*. 2000;24:493–496.
12. Tian S, Nishida Y, Isberg B, et al. MRI measurement of normal extraocular muscles and other orbital structures. *Graefe Arch Clin Exp Ophthalmol*. 2000;238:393–404.
13. Detorakis ET, Engstrom RE, Straatsma BR, et al. Functional anatomy of the anophthalmic socket: insights from magnetic resonance imaging. *Invest Ophthalmol Vis Sci*. 2003;44:4307–4313.
14. Pirouzian A, Scher C, O'Halloran H, et al. Ahmed glaucoma shunt implants in the pediatric population: the use of magnetic

resonance imaging for surgical approach to reoperation. *J AAPOS*. 2006;10:340–344.
15. Ceballos EM, Parrish RK II. Plain film imaging of Baerveldt glaucoma drainage implants. *Am J Neuroradiol*. 2002;23: 935–937.
16. García-Feijoó J, Guiña-Sardiña R, Méndez-Fernández C, et al. Peritubular filtration as cause of severe hypotony after Ahmed shunt implantation for glaucoma. *Am J Ophthalmol*. 2001;132: 571–572.
17. Carillo MM, Trope GE, Pavlin C, et al. Use of ultrasound biomicroscopy to diagnose Ahmed shunt obstruction by iris. *Can J Ophthalmol*. 2005;40:499–501.
18. Jeon TY, Kim HJ, Kim ST, et al. MR imaging features of giant reservoir formation in the orbit: an unusual complication of Ahmed shunt implantation. *Am J Neuroradiol*. 2007;28: 1565–1566.
19. Netland PA, Schuman S. Management of glaucoma drainage implant tube kink and obstruction with pars plana clip. *Ophthalmic Surg Lasers Imaging*. 2005;36:167–168.
20. Singh K, Eid TE, Katz LJ, et al. Evaluation of Nd:YAG laser membranectomy in blocked tubes after glaucoma tube-shunt surgery. *Am J Ophthalmol*. 1997;124:781–786.
21. Valimaki J, Tuulonen A, Airaksinen PJ. Capsule excision after failed Molteno surgery. *Ophthalmic Surg Lasers*. 1997;28: 382–386.
22. Alperin NJ, Lee SH, Loth F, et al. MR–Intracranial Pressure (ICP): a method to measure intracranial elastance and pressure noninvasively by means of MR imaging: Baboon and Human Study. *Radiology*. 2000;217:877–885.
23. Lee JH, Lee HK, Kim JK, et al. CSF flow quantification of the cerebral aqueduct in normal volunteers using phase contrast cine MR imaging. *Korean J Radiol*. 2004;5:81–86.

